Transportation Research Part D 108 (2022) 103332

Contents lists available at ScienceDirect

Transportation Research Part D

journal homepage: www.elsevier.com/locate/trd

Will river floods 'tip' European road networks? A robustness assessment

Kees C.H. van Ginkel [a,b,*], Elco E. Koks [b,c], Frederique de Groen [a], Viet Dung Nguyen [d], Lorenzo Alfieri [e]

[a] Deltares, Delft, the Netherlands
[b] Institute for Environmental Studies (IVM), VU University, Amsterdam, the Netherlands
[c] Environmental Change Institute, Oxford University, Oxford, United Kingdom
[d] GFZ German Research Centre for Geosciences, Section Hydrology, Potsdam, Germany
[e] CIMA Research Foundation, University Campus of Savona, Savona, Italy

ARTICLE INFO

Keywords:
River floods
Road disruption
Road network
Robustness
Resilience
Tipping points
Percolation analysis

ABSTRACT

River flooding is a profound climate hazard in Europe and a threat to its road transport infrastructure. However, its impact on road network interruptions is mostly unexplored, while some have suggested that national road networks may experience tipping points. This study assesses the robustness of road networks of European countries and their potential for a tipping point: an abrupt and disproportionally large loss of network functionality, due to unfavourable combinations of floods. Methodologically inspired by percolation analysis, ten-thousands of flood combinations are sampled and their impacts on road network performance are assessed. The results show that Albania, Croatia, Serbia and Austria are relatively vulnerable, whereas Belgium, Estonia, Lithuania and Portugal are relatively robust. Tipping points in the sense of nationwide network fragmentation seem unlikely, but regional-scale tipping points can happen. Flood-proofing the identified weak spots could result in quick wins for national road operators.

1. Introduction

The world is facing an increase in climate extremes, and the socio-economic consequences of these are increasingly felt (IPCC, 2014). For example, multiple regions across central and western Europe were hit by substantial pluvial and fluvial flooding in July 2021. It is estimated that for the flood events that occurred in Germany, Belgium and The Netherlands, the occurrence of such events has become 1.2–9 times more likely today than in the 1.2 °C cooler pre-industrial climate (Kreienkamp et al., 2021). Such flood events can have a disruptive impact on the road network with profound socio-economic consequences (Hallegatte et al., 2019; Wang et al., 2019). For example, in the German Ahr Valley, many roads and nearly all bridges were severely damaged during the recent July 2021 floods, hampering crisis response, reconstruction work, and economic recovery of the region (GEER, 2021, in preparation). Wang et al. (2019) even suggest that increasing precipitation "may lead to a large-scale systematic malfunction of the entire road network at a critical point" (p. 1). Such critical thresholds, also known as tipping points, are a reason for concern because they indicate that a gradual climate forcing may have abrupt, disproportionally large impacts on the economy and society.

Flood-induced road damages and the resulting societal impacts have been studied from various perspectives and spatial scales

* Corresponding author at: Deltares, Boussinesqweg 1, 2629 HV Delft, the Netherlands.
E-mail address: Kees.vanGinkel@Deltares.nl (K.C.H. van Ginkel).

https://doi.org/10.1016/j.trd.2022.103332

Available online 2 June 2022

(Wang et al., 2020; Zhang and Alipour, 2020). Highly detailed studies describe the mechanisms causing physical road damage – such as bridge scour (Wang et al., 2017) and embankment failure (Johnston et al., 2021; Pedrozo-Acuña et al., 2017). Other studies have focused on physical asset damage on different spatial scales such as cities (Nicklin and Dieperink, 2019; Pregnolato et al., 2017), river basins, or even continental and global (Koks et al., 2019; van Ginkel et al., 2021b; Mulholland et al., 2021). Moreover, an increasing number of nation-wide infrastructure stress tests have been done (e.g. Canada: Palko and Lemmen, 2017, Netherlands: de Grave et al., 2020, Bles and van Muiswinkel, 2019), typically going beyond infrastructural damage by also examining societal impacts such as traffic congestion which is often expressed by vehicle loss hours (Fournier Gabela and Sarmiento, 2020). Some of these use the detailed traffic models that normally support (national) spatial planning, which are rather computationally expensive due to a complex model cascade of trip generation, trip distribution, and a variety of transport mode choices (de Dios Ortúzar and Willumsen, 2009). This level of complexity makes them less suitable for large-scale calculations of many possible flood scenarios. Moreover, many assumptions underlying these models, such as traveller preferences and trip generation, do not fit with a large-scale flood crisis situation (Dong et al., 2020a). Therefore, in this study we adopt a network percolation approach (Abdulla et al., 2019; Dong et al., 2020a), which allows for rapid assessment of many flood events in large networks.

Network percolation is a graph-theoretic approach for the study of tipping points in networks. Originating from physics, where it was used to model tipping-point like phase transitions in materials (Radicchi, 2015), it found wider application to transport networks (Dong et al., 2020b), including a handful of road network studies. Large scale road percolation studies are mostly done without hazard data, and instead use random, localized or probabilistic failure patterns. For example, Arcaute et al. (2016) percolated the British road network to identify hierarchical regional and urban clusters, while Dong et al. (2020a) percolated the networks of 16 United States of America (USA) cities and states to characterize their robustness. Percolation studies with flood hazard data are mostly restricted to a small spatial scale. For example, Abdulla et al. (2019) modelled the fluvial flood vulnerability of a neighbourhood in Houston - USA; Dong et al. (2020b) modelled road-sewer failures in Portland - USA; and Dong et al. (2022) modelled road disruption and traffic congestion in Harris County, Texas - USA. Wang et al. (2019) studied flood disturbances on a large spatial scale, by examining the entire road networks of China and the USA. They suggest that entire national road networks are at risk of large-scale malfunction due to catastrophic floods, which well aligns with concerns about climate change induced socio-economic tipping points, some of which are known to result from network effects (Filatova et al., 2016; Jain et al., 2012; Kopp et al., 2016; van Ginkel et al., 2020).

The objective of this paper is to examine the robustness of the national road networks of thirty European countries and their potential for socio-economic tipping points, i.e. an abrupt and disproportionally large loss of network functionality due to an unfavourable combination of floods. We will briefly touch upon the above 'percolation point' tipping points, but only use these on the side and for reference, because we soon discover that these have little real-world policy relevance. Instead, we focus on policy-relevant tipping points; the importance and originality of our study lies in the increased understanding of their existence. We seek to make two methodological contributions to the literature. First, we examine how realistic it is that catastrophic floods cause tipping points in the performance of national-scale road networks. Second, we explore if an adapted form of percolation analysis can deliver useful results for formulating climate adaptation policy. Before describing the technical specifications of the method (Section 3), we first

Fig. 1. Application of the stepwise approach (van Ginkel et al., 2021a) for tipping point identification and decision support in this study. 'M' denotes a metric.

methodologically consider how policy relevant tipping points can be identified using a stepwise approach (Section 2).

2. A stepwise approach to tipping point identification

Socio-economic tipping points occur when a system abruptly changes into a fundamentally different state upon a relatively small perturbance (Milkoreit et al., 2018; van Ginkel et al., 2020). The variety of tipping point conceptualisations has led to misunderstanding and controversy (e.g. Kopp et al., 2016; Russill and Lavin, 2012; van Nes et al., 2016), because it often remains unclear from what disciplinary perspective, for which stakeholders, and on what spatial and temporal scale something is considered a tipping point (Van Ginkel et al., 2020). The graph-theoretic percolation point is an example of a tipping point that may be easily misunderstood. One may infer from Dong et al. (2022) and notably Wang et al. (2019) that there could be flood events that cause a sudden fragmentation of the entire road network, which prompted our investigation of whether this could also happen to the road networks of European countries. Our results (section SI 3), however, suggest that such tipping points are unlikely to happen with more realistic flood hazard data, as recently also argued by Loreti et al. (2022). Moreover, they seem of little policy relevance because the network functionality is already severely compromised well before the percolation point is reached (Dong et al. 2020a, Loreti et al., 2022). This raises the question if there could be other types of tipping points in national road networks, that do have policy relevance.

To investigate policy relevant tipping points, this paper uses the stepwise approach of van Ginkel et al. (2021a, under review) to give insight into the assumptions underlying tipping point assessment and to clarify the applicability, validity and scope of the results (Fig. 1). Thereby, we aim for a transparent and reproducible study design that deliver policy-relevant insights.

The stepwise approach is shown in Fig. 1. Our study defines a tipping point as an abrupt, disproportionally large loss of functionality of a road network system of an entire country during a river flood event, measured by three metrics (M) for system-wide performance (step 1–2, Fig. 1). Step 3 operationalises this tipping point in two ways, reflecting two perspectives. Firstly, we operationalise a tipping point as a large river flood event (at multiple locations at the same time) that disrupts routes between major economic centres beyond acceptability thresholds defined in Section 3.1.4. Secondly, we operationalise a tipping point as a high-likelihood, small-scale flood event that causes an outlier in the metrics. These are tipping points because of their disproportional large impact on the network compared to other events in the country with comparable magnitude and likelihood.

Step 4 identifies the tipping points among the many possible combinations of concurrent floods, using a random sampling scheme (Section 3.1, Section 4.1) and a guided sampling procedure (Section 3.3, Section 4.2). Step 5 and 6 are covered in the discussion (Section 5) and conclusion (Section 6).

3. Method

This section details the set-up of the random percolation analysis (Section 3.1), the sensitivity analysis (Section 3.2) and the guided sampling analysis (Section 3.3), which elaborate the steps of Fig. 1.

3.1. Default model set-up: Random sampling

3.1.1. Network exposure

This study examines the European road network, meaning that other transport modalities such as rail, inland waterways, and air transport are excluded. The road network is cut along country borders and includes all motorways, trunk roads, primary, secondary and tertiary roads in OSM (OpenStreetMap) on December 1st, 2020 (OpenStreetMap contributors, 2020), see Fig. 2, panel 1 for a stylized overview and Figure SI 1–30 for a description of each country's data. As a proxy for the most important within-country connections, we analyse the routes between the regions at the level 3 or 2[1] of the NUTS (Nomenclature of Territorial Units for Statistics) regions, which split Europe into spatial economic units (Eurostat, 2016), see Fig. 2, panel 2. This allows for mutual comparison of countries while reflecting a birds-eye transport-economic actor perspective on network robustness (Fig. 1, step 1).

To reduce graph complexity, consecutive road segments without crossroads (i.e. graph nodes with degree 2) are merged without a reduction of geometric network detail. The centroids of NUTS-regions are assigned to the nearest distance network vertices as the trip origins and destinations (Fig. 2, panel 2). Route choice is based on shortest travel time using the Dijkstra algorithm as implemented in the Python-iGraph package (Csardi and Nepusz, 2006). The entire code base, input data and scripts for figure reproduction are openly available, see 'Data and code availability'.

3.1.2. Flood hazard

We use the LISFLOOD-FP 100-year return period flood map of Europe, consisting of river floods with upstream catchments larger than 500 km^2 (Dottori et al., 2021). This map is decomposed in smaller chunks, further referred to as 'microfloods' throughout this paper. Each microflood is a 100 * 100 m^2 resolution flood extent and water depth raster of a few kilometre width and height (Fig. 2, panel 4-top). These microfloods result from a 1:100 year river discharge hydrograph in a corresponding 5*5 km^2 grid cell of the LISFLOOD hydrological model. Therefore, each high-resolution microflood can be seen as originating from the so-called 'Area of Influence' of the 5*5 km^2 grid cell of the hydrological model (Alfieri et al., 2015), which in principle can reach outside the 5 * 5 km^2

[1] [1]Aiming at a consistent increase of number of NUTS-regions by country size (Table 1) and to reduce computational time we use NUTS-2 instead of NUTS-3 regions for Belgium, The Netherlands, United Kingdom, Italy, Germany.

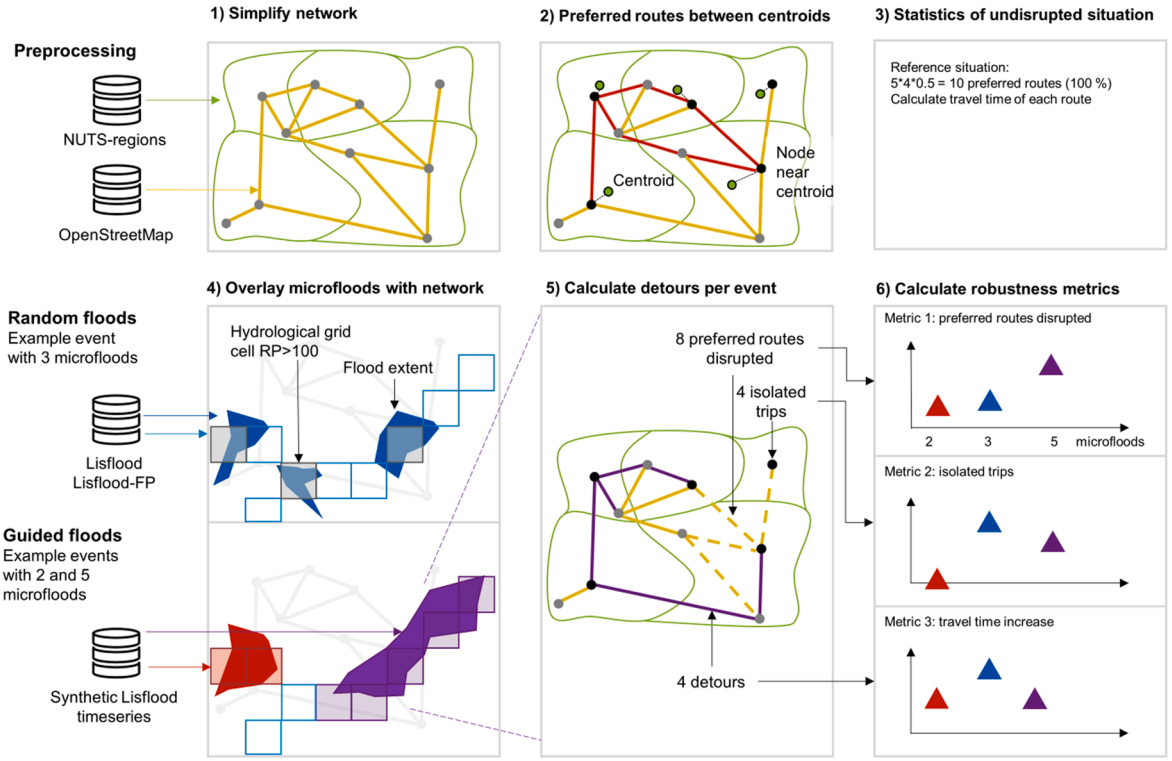

Fig. 2. Stylized overview of the analysis for a hypothetical network and data. Panels 1–3 show the preprocessing steps that are done once for each country. Panels 4–6 show the percolation processes, which is repeated 200 times to create events for each number of microfloods (x-axis of panel 6). Panel 4-top illustrates random flood event generation with one example event (blue) (Section 3.1); 4-bottom illustrates guided flood event generation with two example events (red, purple) (Section 3.3). Panel 5 demonstrates the alternative route choice during the purple flood event. Panel 6 shows how the robustness metrics are derived and visualised. (For interpretation of the references to colour in this figure legend, the reader is referred to the web version of this article.)

grid cell, see Fig. 2, panel 4-top. To determine which roads are flooded during which microflood, we spatially overlay the hazard data with each road segment and add the flood depth as metadata to each road segment, for details see van Ginkel et al. (2021b).

A critical element in percolation analysis is the sampling of combinations of microfloods that may happen simultaneously during an event. In a default percolation analysis, one would randomly remove segments one-by-one, including segments that are not exposed to floods. In contrast, we remove all segments hit by one microflood at once. However, the sampling of concurrent microfloods may still be random (Section 3.1, Section 3.2, Section 4.1) or guided by a correlation structure (Section 3.3, Section 4.2). For random sampling, assume a country with a total of T microfloods, of which we sample k at the same time to form a flood event. There are $N = \binom{k}{T}$ combinations N when sampling k events, of which a subset $n = 200$ per k value is sampled, which proved to be sufficiently large to gain a robust 95% confidence interval of results (section SI 4).

3.1.3. *Network impact assessment*

For each flood event, the network performance is assessed with three metrics. The first metric (M1) *preferred routes disrupted* measures the number of trips (between origin–destination pairs) for which the preferred route (shortest travel time) is disrupted. The origin and destination may still be connected through alternative routes, but capacity constraints may be expected on these detours. The second metric (M2) *isolated trips* measures the number of trips (origin–destination pairs) that are no longer connected. For these trips, not only the preferred route is disrupted, but also no alternative route remains. The third metric (M3) *travel time increase* measures the average increase of travel time of the remaining (disrupted but not isolated) trips. Note that these metrics are different from and more sensitive than the classic 'giant component size' metrics of default percolation analysis, see section SI 3.

3.1.4. *Tipping point identification*

For each number of microfloods k (x-axis, Fig. 2, panel 5), the analysis returns $n = 200$ metric scores: one score for each sampled event (y-axis). By taking summary statistics at each point k, each country obtains a robustness curve that indicates the decline of network performance (y-axis) for increasingly large flood events (x-axis), see Figs. 3 and 4. A steeper curve indicates a less robust network. There are two ways to define and identify tipping points from these curves (Fig. 1, step 4).

Firstly, on the national scale, a tipping point is the number of microfloods (x-axis) at which the disrupted routes or isolated trips metric (y-axis) exceeds a stakeholder-defined threshold value, which is subjective but could for example be: 50% of *preferred routes*

Table 1
Summary statistics of country, road network, flood hazard and percolation analysis, sorted by country area. (1) Only includes the land area of NUTS-regions that can be reached from the largest connected land area, without crossing country borders or water. (2) For countries with a *, we took NUTS-2 regions (and show the number of NUTS-3 region between brackets), for all other countries, we took NUTS-3 regions. (3) OSM road types: motorway, trunk, primary, secondary and tertiary (4) Length of the network edges that may be (partly) inundated, as a percentage of total network length (5) For correlation plots for absolute and relative scores, see Figure SI 31

Country	Area[1]	# NUTS-regions[1,2]	Total network length[3]	Potential inundated share of network[4]	M1: Preferred routes disrupted, worst 5% disruptions at single microfloods[5] $M1_{k=1,P=95\%}$	M1: Preferred routes disrupted, mean disruption at 5 (and 5%) microfloods[5] $M1_{k=5,mean}$ ($M1_{k=5\%,mean}$)	M2: Worst 5% isolated trips at 10 (10%) microfloods[5] $M2_{k=10,P=95\%}$ ($M2_{k=10\%,P=95\%}$)
	km^2	–	km	%	%	%	%
Slovenia	20,272	12	10,239	24.0	41	24 (30)	17 (77)
Macedonia	25,434	8	8373	27.0	32	27 (37)	0 (78)
Albania	28,800	12	8221	33.2	36	33 (51)	17 (86)
Belgium	30,666	11* (44)	34,896	14.9	13	10 (17)	18 (54)
Netherlands	37,380	12* (40)	43,482	29.9	23	22 (32)	17 (69)
Switzerland	41,286	26	25,766	22.1	13	15 (34)	8 (72)
Denmark	43,171	10	37,040	2.8	4	6 (5)	20 (53)
Estonia	45,345	5	16,234	14.4	20	11 (15)	0 (58)
Slovakia	49,024	8	20,051	33.0	25	22 (53)	0 (89)
Croatia	54,740	21	31,087	27.5	34	26 (60)	10 (85)
Latvia	64,587	6	24,913	24.4	7	10 (36)	2 (84)
Lithuania	64,897	10	23,774	18.7	11	9 (24)	0 (66)
Ireland	69,940	8	39,282	11.4	14	14 (25)	25 (64)
Serbia	77,488	25	20,511	48.3	28	20 (63)	8 (87)
Czechia	78,873	14	61,203	13.1	15	11 (35)	0 (78)
Austria	83,945	35	45,022	22.6	25	18 (55)	11 (84)
Portugal	88,786	25	63,759	10.8	16	12 (36)	0 (69)
Hungary	93,009	20	36,362	34.6	7	6 (33)	0 (69)
Bulgaria	110,994	28	25,511	30.4	8	9 (39)	0 (74)
Greece	111,361	52	82,139	10.4	25	14 (47)	0 (79)
United Kingdom	224,768	40* (1 7 9)	167,507	10.0	7	6 (40)	0 (72)
Romania	238,368	42	70,857	30.5	7	8 (61)	0 (87)
Italy	250,811	19* (1 1 0)	228,749	16.3	25	12 (76)	11 (94)
Poland	311,941	73	151,014	19.5	2	5 (50)	0 (81)
Norway	323,335	18	63,206	28.3	17	14 (69)	12 (94)
Finland	336,166	19	84,933	32.5	3	7 (49)	11 (79)
Germany	357,661	38* (4 0 1)	284,400	17.3	3	2 (45)	0 (75)
Sweden	446,478	21	112,649	27.4	27	5 (60)	0 (87)
Spain	493,529	59	233,138	15.9	5	4 (56)	0 (86)
France	540,213	94	468,130	14.6	7	4 (62)	0 (87)

disrupted (M1), 10% *isolated trips* (M2), and/or 3 h average *extra detour time* (M3). Because there is some subjectivity in the precise position of these thresholds, we judge tipping point susceptibility in a relative sense, by mutually comparing country scores and curve shapes. For example, a country with a steeper curve is more likely to exhibit tipping points than a country with a flatter curve, irrespective of where the tipping point threshold precisely lies (see result Section 3.1).

Secondly, a tipping point is an outlier event (unusually high M1, M2, or M3 for given k), where a flood causes disproportionally large network disruption compared to other events of the same magnitude (k). Formally, the upper outliers in the boxplot visualisations in this paper are defined as the points past the upper whisker of the box-and-whisker plot, which lie more than 1.5 * (Q3-Q1) above the Q3 quartile value. Note that in both definitions, the network reconfiguration is not persistent as road operators will seek to restore the inundated or broken road segments in the direct aftermath of the disaster.

3.2. Sensitivity analysis of default set-up

To assess the sensitivity of the results to our model assumptions, we vary the setup of the random percolation analysis as described in the supplementary information (section SI 4). For each variation of model set-up, we assess the impact on the metric scores for Belgium, a relatively small country with a substantial flood hazard and a sufficiently complex road network, which could be run within a reasonable amount of computational time. If we have a strong suspicion that other countries might behave different from Belgium, we also assess the sensitivity for additional countries. The results can be found in section SI 4.

3.3. Alternative model set-up: Guided sampling in Germany

In contrast to random sampling, guided sampling uses the spatial dependence structure of the annual maximum streamflow timeseries to determine which microfloods may concur during an event (Fig. 2, panel 4-bottom). The spatial dependence structure is derived from 141 gauging stations in Germany, based on continuous daily discharge data from Global Runoff Data Centre (2020) for a common, 41-year time period (1965–2005). A multivariate student-t copula model represents the spatial dependence along the river network during hydrological extremes (Nguyen et al., 2020). The station selection and geo-location matching steps are based on criteria described in Nguyen et al. (2020), which also describes the Student-t copula multivariate model. This model was used to generate 10,000 years of annual maximum return period values for each of the 141 discharge stations.

To apply the discharge station data to flood events covering entire Germany, the following assumptions were made. First, the annual maximum discharge is assumed to occur during the same flood event at all stations. This is a worst-case assumption because a part of the stations could for example reach their annual maximum during an event in spring, whereas the rest could experience it in the autumn of the same year. Second, we assumed that if a station measures a flood peak of a certain return period, all grid cells located downstream along the river network until the following station have the same return period. For the most upstream stations of each river basin, the same dependence is propagated upstream until the headwaters of the river network. This also is a worst-case assumption, because under some conditions a dike breach at one location could reduce the flood volume (and thus the return period of the discharge) downstream. In contrast to the set-up of the random percolation, inundation depths and extents at each grid cell are taken from the raster that best matches the modelled return period, from the available 10, 20, 50, 100, 200 and 500 year return period simulations. In the same spirit, we do not assume fixed dike breaches at the 100 year return period as in the random percolation, but account for the local flood protection levels in place (after Dottori et al., 2021). Hence, a road segment is only removed from the network if the flood return period exceeds the flood protection in place.

4. Results

4.1. Random percolation analysis

This section presents the results of the percolation analysis with random flood sampling. For each country, a dashboard with a network map and metric scores is provided in the Supplementary Information (Figure SI 1–30).

4.1.1. A helicopter view of the road networks of 30 European countries

A summary of the network robustness and geospatial country characteristics is provided in Table 1. A first trend in Table 1 is that the percentage of *preferred routes disrupted* (M1) by a single microflood (k = 1), roughly decreases for increasing country size. This indicates increasing robustness against these 5% least favourable single microfloods (Table 1). The top-3 smallest countries Slovenia, Macedonia and Albania are in the top-4 of the *preferred routes* indicator; the 5% worst single microfloods in these countries can disrupt 32–41% of the preferred routes (see also Figure SI 31a). In contrast, one unfavourable microflood in Germany or Finland can disrupt around 3% of the preferred routes. A second trend is that scores increase for countries with a large potential inundated share of the network, indicating decreasing robustness for more flood-prone countries.

The percentage of *preferred routes disrupted* (M1) at an absolute number of five microfloods (k = 5), roughly has the same pattern: smaller countries are less robust than large countries (Table 1, Figure SI 31b). The small country Albania scores worst (33%), while Germany as one of the largest countries scores best (2%). However, there are interesting deviations from this pattern. For example, Belgium is relatively robust (10%) for a small country, while Norway is relatively vulnerable for a large country (14%). For Belgium, the relatively low potential inundated share of the network seems to be an explanatory factor for the low score. The percentage of *isolated trips* (M2) at ten microfloods (k = 10) seems to have some correlation to the *preferred routes disrupted* (M1), but not very strong.

These results suggest that country size plays an important role in the metric scores. The next subsection will therefore mutually compare countries of comparable size and explore whether the remaining differences can be explained from network topology and flood characteristics. Also, the next subsection will examine the relative percentage of total microfloods per country, instead of the absolute number of microfloods.

4.1.2. *Differences and similarities between countries of comparable size*

This subsection seeks to explain the differences and similarities between countries of comparable size through geospatial, network topology and flood hazard characteristics. The groups and metric scores are shown for *preferred routes disrupted (M1)* (Fig. 3) and *isolated trips (M2)* (Fig. 4); the *extra travel time* (M3) results can be found in Figure SI 32. Note that in these figures, the maximum value on the x-axis (100%) denotes that all possible microfloods are occurring ($k = k_{max}$) and that the maximum potential inundated share of the network indicated in Table 1 (e.g. 30.5% for Romania) is reached. Because not every single road segment is exposed to river floods, there is a (small) chance that a preferred route, consisting of many segments, remains completely unaffected. This explains why at 100% of microfloods, M1 is often below 100% (Fig. 3). Moreover, there is (larger) chance that alternative routes between origin and destination remain, even for very large floods. This explains why at 100% of microfloods, M2 is often well below 100% (Fig. 3).

When comparing the different groups in *preferred routes disrupted* (M1, Fig. 3), it appears that the percolation curves roughly have an exponential shape. The curves of larger countries are generally steeper. This result may be explained by the larger total number of microfloods and trips that larger countries have, meaning that in a larger country, the same relative percentage corresponds to a larger number of absolute number of floods, which combined effect apparently is more disruptive. At the same time, the confidence intervals of smaller countries are larger, indicating that the least favourable small-scale floods in smaller countries are more destructive than in larger countries.

The *isolated trips* curves (M2, Fig. 4) have more diverging shapes and larger bandwidths than M1. The incidental up-and-downward spikes in the bandwith are a consequence of the random sampling procedure. Although there is a clear increasing trend in all M1 and M2 scores (Figs. 3, 4) for increasing numbers of microfloods k, sometimes the 200 realisations of a smaller k-value by chance contain more extreme outliers than the 200 realisations of a larger k-value. Section SI 4.1 shows that this mainly effects the tail of the distribution.

The *travel time increase* of the detours (Figure SI 32) reaches up till 4 h for the smaller countries (group I-III), and up till 10 h for the larger countries (group V-IV). The larger countries have larger networks, which provide more detour possibilities at the cost of large detour times. Consequently, this metric shows that a low chance of trip isolation (low M2-score) sometimes comes at the price of very long detour times (high M3-score), for example in Spain, France, Italy and Bulgaria. Another characteristic is that many M3-curves at some point start decreasing for large x-values, some clear examples are Slovakia, Serbia and Norway (Figure SI 32). This contrasts to M1 and M2, which are increasing over the entire domain. The explanation lies in M3′s definition as the *average* travel time increase of the routes *with* detour, i.e. the not isolated trips. In some cases, the average detour time first increases due to some very long (above average) detours, and then starts to decrease when these are no longer possible.

In group I, the smallest country Albania is the least robust, scoring worst on all metrics in both absolute (number of microfloods)

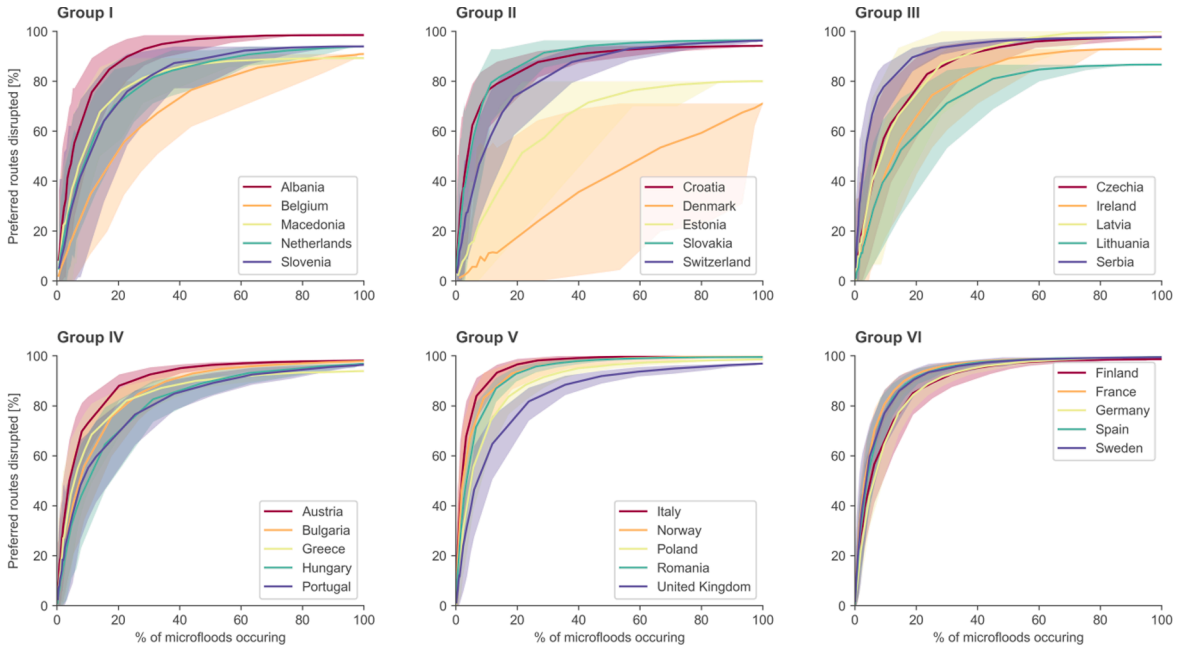

Fig. 3. Disruption of preferred routes between NUTS-regions due to combinations of river floods. Grouping is based on ascending country area. The solid line indicates the mean, and shaded area the 90% interval.

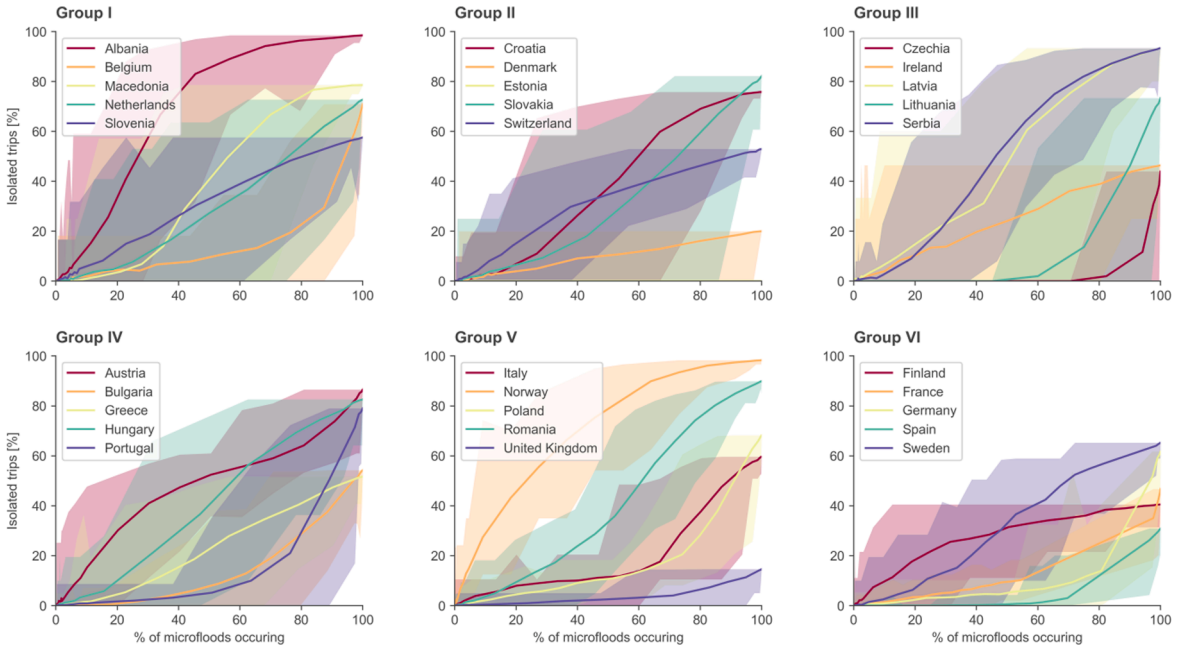

Fig. 4. Number of isolated trips, i.e. with no possible path between origin and destination, between NUTS-regions due to combinations of river floods. Grouping is based on ascending country area. The solid line indicates the mean, and shaded area the 90% interval.

and relative (percentage of microfloods) terms (Fig. 3, 4, SI 3). The eastern part of Albania is mountainous, and the routes through the country heavily rely on one North-South corridor in the flatter Western part (Figure SI 3). Floods can disrupt this corridor at several places, causing disruption of many preferred routes, detours with very large travel times, and relatively easy isolation of remote areas. Somewhat similar, Macedonia and Slovenia are mountainous with a higher risk of regional isolation. In contrast, Belgium and The Netherlands are relatively flat and have more extensive road networks (Table 1). They are relatively robust against *disruption of preferred routes* and even more against *isolated trips*. Belgium is more robust than the Netherlands, because it is less exposed to large-scale river floods (Table 1). However, the sensitivity analysis shows that Belgium also has a more vulnerable northern part, Flanders, which is compensated by a more rubust southern part, Wallonia (section SI 4.3). This is an important observation, because it shows that local weaknesses may remain unnoticed in the nation-wide metrics.

Group II has two countries with atypical curves that indicate large robustness: Estonia and Denmark. Both networks have low exposure to large-scale river floods, because there are few substantial rivers and because catchments below 500 km^2 are not in the hazard data (Section 3.1.2). As a result, the *preferred routes disrupted* (M1) curve is relatively flat and does not go above 80% (Estonia) and 71% (Denmark). Also in absolute terms, Estonia and Denmark are relatively robust (Figure SI 7, SI 8). Estonia has no routes without detour (M2). The beginning of the Switzerland *isolated trips* (M2) curve is rather steep, because some centroids are located in remote mountainous places which can easily become isolated because they can only be reached through one road (Figure SI 6). Overall, Slovakia and Croatia the least robust, including long *extra travel times* (M3, Figure SI 32). In Group III, Serbia has the least robust network and the highest percentage of potentially inundated network of all 30 countries (Table 1), which aligns with its reputation of being flood-prone (Gavrilović et al., 2012). The Achilles' heel is the central A1 highway in the floodplains of the Danube and Morava rivers (Figure SI 14), which is used for many preferred routes. Where possible, detouring in Serbia comes with long additional travel time. Having only six NUTS-3 regions, Latvia has a relatively large confidence interval (Figure SI 11) indicating a substantial risk that major economic centres area are affected despite reasonable overall robustness. Ireland is rather robust because of limited flood exposure. At the same time, the floods that can occur are among the most disruptive in the group (Figure SI 3). Lithuania and Czechia are the most robust of their group, especially the risk of *isolated trips* (M2) is rather small.

In group IV, Austria scores notably poor on all metrics. The country dashboard (Figure SI 16) shows two peculiarities of the network. First, the road density is high in the flatter north and south-east, but very low in the mountainous west and centre of the country. Second, the regions Tirol and Voralberg, that stick out at the west, are only connected to the rest of the country with a handful of primary roads, none of which are mapped as motorways or trunk roads in OpenStreetMap. The main road connection with Tirol goes through neighbouring country Germany. In contrast, Portugal scores reasonably well (Figure SI 17) because the overall flood exposure is low (Table 1). A few substantial rivers can disrupt important corridors in the west of the country, but much redundancy remains so that trip isolation only sharply increases during very large floods (Fig. 4). Bulgaria has a relatively small road network, given the area of the country. Nevertheless, it scores good on *disruption of preferred routes* (M1), and even better on *routes without detour* (M2), because of the favourable (relatively square) ratio between length and width of the country, which makes it unlikely that regions become isolated because of the many possible remaining detour options. Note that the absence of *routes without detour* (M2) causes a strong increase of *extra travel time* (M3) over the network during flood events (Figure SI 19). In Greece, the *extra travel time* (M3) also sharply

increases, possibly because the Peloponnese peninsula (in the South) is connected to the North through two alternatives, which are more than 100 km apart (Figure SI 20).

In group V, Italy shows a sharp increase of *disruption of preferred routes*, due to a combination of (a) its boot shape – which makes that many origin–destination pairs use the same route and road segments, and (b) the fact that these segments are exposed to a large flood hazard, notably in the Po River Valley in the North of the country (Figure SI 23). At the same time, there is enough redundancy to avoid large-scale trip isolation up till 60% of all microfloods (Fig. 4), albeit at the cost of large extra travel time. In contrast, large-scale trip isolation seems more likely in Norway, another very elongated country. Norway has a substantial risk that the northern NUTS-3 regions may become isolated from the rest because they are only reachable through one north–south corridor (Figure SI 25). This effect is partly a model artefact, because detours through neighbouring country Sweden are reasonable alternatives that are not considered in our approach. Also, we need to report on a limitation of the hazard data: recent research shows that the river flood risk in Scandinavian countries tends to be overestimated by the model we used (Dottori et al, 2021, under review). An interesting pair of countries is Romania and Poland: both have a favourable ratio between length and width and the number of NUTS-regions and network length is not very large compared to the country size. However, the network of Romania is more exposed to floods than the network of Poland (Table 1), which strongly decreases the network robustness as indicated by higher scores on all three metrics, notably the *extra travel time* (Figure SI 22).

In group VI, Finland and Sweden seem to be the least robust, with especially Finland scoring poor on isolated trips. Their patterns resemble Norway, with moderate scores on *preferred routes* (M1) and poor scores on *isolated trips* (M2), which can be explained from large exposure to floods in the hazard data. France, Germany and Spain score well on M1 and M2. In Spain and France, this comes with large travel time for large floods. Germany is very robust against disruption of preferred routes, but for extremely large floods (greater than 60% of all microfloods) the risk of trip isolation (Figure SI 27) is quickly growing to ultimately well above France and Spain.

4.1.3. Examples of disruptive outliers

While the country-level comparison in Section 4.1.1 and 4.1.2 provides insight into the general robustness of country-level networks and nation-wide tipping point susceptibility, it pays little attention to outliers. These outliers are defined as the second type of tipping points, as relatively small flood events with a disproportional (and unusual) large impact on the network performance. Here, two examples are illustrated.

Fig. 5 shows the most severe microflood in Albania, causing the largest disruption of preferred routes (panel c) and a large increase of travel time over the network (panel e). It does not cause any isolation of trips.

Fig. 6 shows the most severe microflood in Austria, causing isolation of 5 regions in Tirol and Voralberg (west of the country), because traffic over the borders is not considered. Note that the travel time does not increase (panel e), because for none of the disrupted routes a detour is found. This case raises the question how sensitive the results are to assumptions in the model-setup,

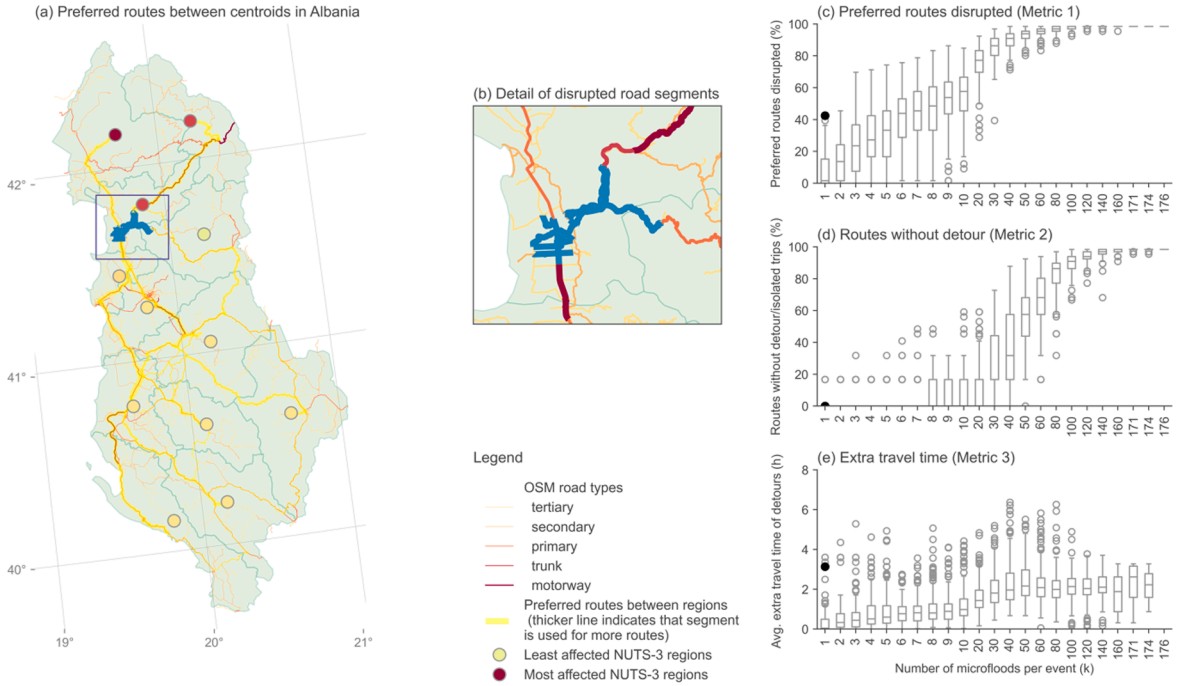

Fig. 5. Microflood event (indicated by the black point in panels c-e) that causes disproportionally large disruption of preferred routes (panel c) in Albania, and a large increase of travel time over the network (panel e). Road geometries ©OpenStreetMap contributors, distributed under a CC-BY license.

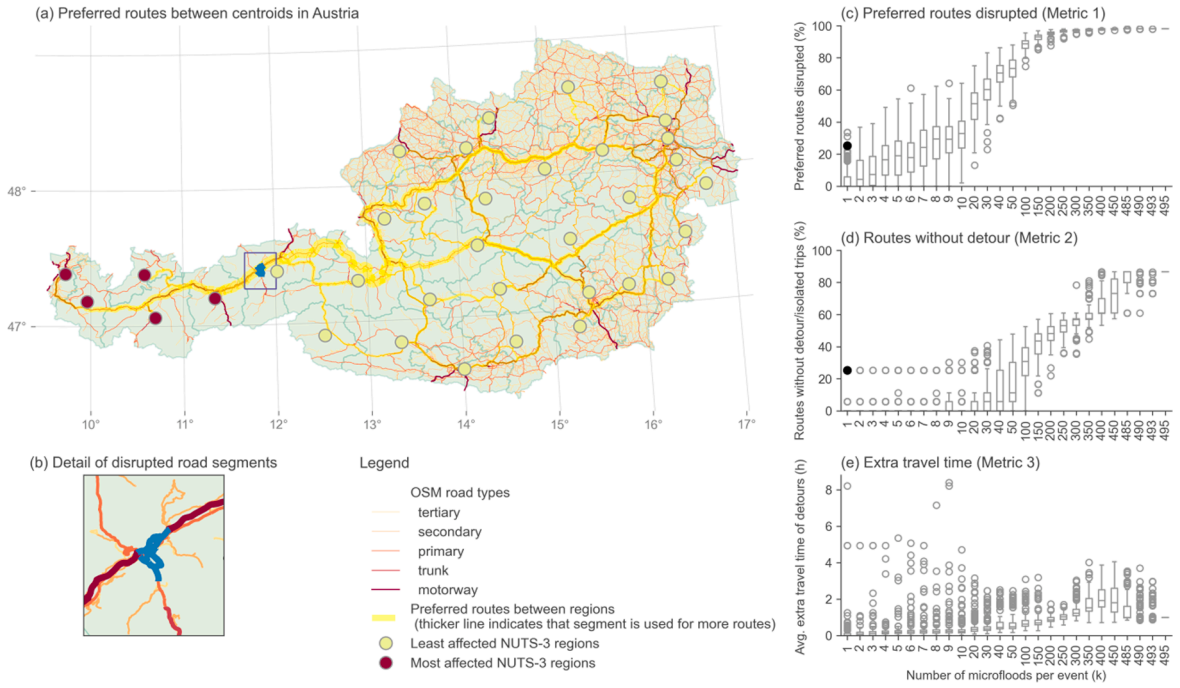

Fig. 6. Microflood event (indicated by the black point in panels c-e) that causes disproportionally large isolation of regions in the west of Austria (panel d). Travel time over the network does not increase because no alternative routes were found for disrupted preferred routes, assuming that no traffic over the borders is possible. Road geometries ©OpenStreetMap contributors, distributed under a CC-BY license.

because these regions would not be so easily isolated if the road network of neighbouring countries would have been included. Section SI 4.2 shows that Austria indeed scores significantly better (lower) on *routes without detour* (M2) when allowing for detouring through neighbouring countries.

4.2. *Guided percolation in Germany*

Fig. 7 shows how the results of the guided sampling compare to the random sampling. The pattern of the sampled results is revealing in several ways. Most striking is that for larger sampled floods, $k > 200$ microfloods, the M1-scores are consistently below the randomly sampled floods of similar size (panel a). The explanation is that the events generated in the guided sampling are strongly spatially correlated, i.e. the floods all happen in the same part of the country and hit a delineated subpart of the network while leaving

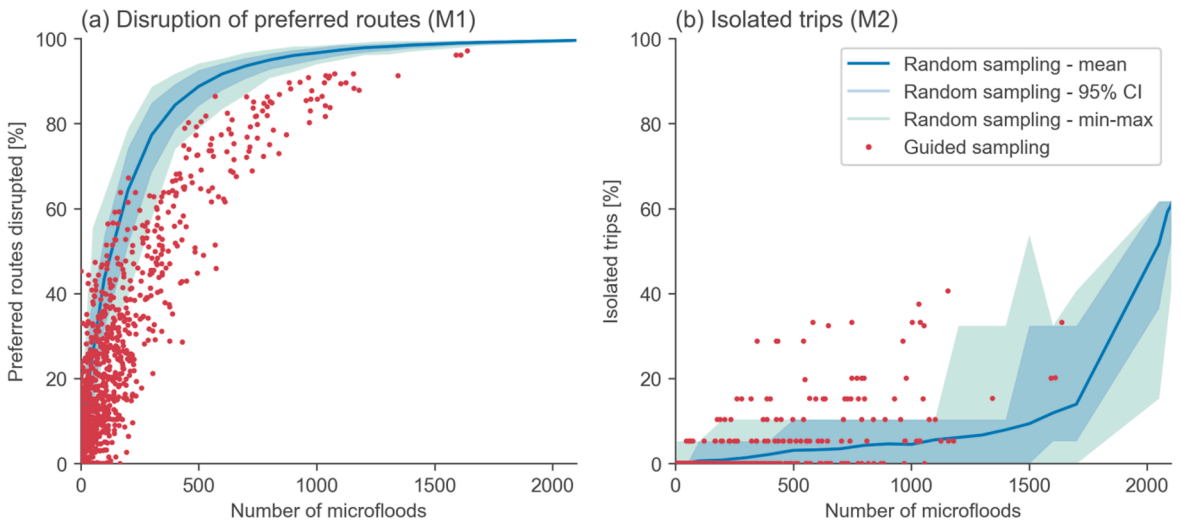

Fig. 7. Guided sampling based on (Nguyen et al., 2020), compared to random sampling as in Section 4.1.

the rest of the network intact. As a result, many floods in the guided sample hit the same route. In contrast, the random samples are randomly scattered over the country, which increases the likelihood of hitting different routes instead of the same route.

At the same time, the M2-scores are often higher in the guided sampling (Fig. 7, panel b). The likely explanation is that the origin and destination points are more easily isolated because locally, the floods are more severe. Apparently, the chanches are low that such locally destructive floods are identified in the random sampling. This is also found by Wang et al. (2019).

Note that the guided sampling used the actual flood protection in place, instead of a uniform 1:100 year protection level such as in the random sampling. This explains the relatively high metric scores for guided sampling at some low numbers of microfloods: these are the few locations in Germany where the flood protection is below 1:100 year, and no flooding was predicted in the random sampling.

Despite being more realistic than random sampling, still worst-case assumptions were taken in the guided sampling (see Section 3.3). With that note of caution, we may count the number of extremely disruptive events to gain a first impression of the maximum frequency of nationwide tipping point-like events in Germany in the current climate, knowing that with more realistic assumptions the frequency will be lower (return period larger). For example, the maximum frequency of an event disrupting $\geq$ 50% of preferred routes (M1) is 0.016 year^{-1}, i.e. a minimum return period of 63 years. The frequency of an event making $\geq$ 10% of trips impossible (M2) is at maximum 0.006 year^{-1}, i.e. a minimum return period of 179 years.

5. Discussion

The answer to 'will river floods cause tipping points in European road networks?' depends on the system scale and actor perspective (as in: the choices made in steps 1–3 of the stepwise approach, Fig. 1). How about the first type of tipping points - the crossing of acceptability thresholds – that reflect a national transport-economic perspective? In most countries, the majority of flood events with a size of 10% of all microfloods disrupt more than 50% of all preferred routes (Fig. 3), according to random sampling. The guided sampling for Germany implies a maximum annual likelihood in the order of 2% for this traffic-chaos tipping point in the current climate. In practice, this likelihood will be lower because we took many worst-case assumptions. Hence, it seems that the outlier events, the second tipping point type, have more policy relevance. The fact that the 5% least favourable individual *single microfloods* may already disrupt up till 41% of preferred routes between major economic centres in a country is rather disturbing, because of its substantial probability and major impact: severe disruption of traffic. This is also displayed by the large extra travel times caused by some unfavourable floods, which would have been worse if traffic congestion had been accounted for. To put this in perspective: the road operator of the Netherlands indicated that a few unfavourable events in a row can mean a tipping point for their operations because of societal unrest about the resulting traffic chaos (see SI to Van Ginkel et al., 2020).

The societal impacts of regions that become temporally isolated from the network may be severe. The risk is already substantial for some countries in the random sampling, and the guided sampling shows that when accounting for spatial correlations it may increase. This could mean that during actual flood events some regions may be hard to reach for emergency responders and that reconstruction works are hampered by disrupted connections. During the Ahr Valley flooding in 2021, the road network was so severely hit that some villages became nearly inaccessible to normal vehicles. Arguably, this event was not a tipping point on the national scale, but nevertheless a tipping point for inhabitants of the valley, who besides the casualties and material losses also experienced a substantial economic shock and a need for a nearly complete reconstruction of transport infrastructure in the area (Koks et al., 2021, under review). In this context, an interesting finding of the present study is that local network weaknesses may remain hidden in the nationwide metrics of larger countries like Germany, meaning that a robust national network is no guarantee that some individual components are still susceptible to (local or regional) tipping points.

Despite the extensive uncertainty analysis, our results must be interpreted with caution. Although the 100 * 100 m^2 flood hazard resolution is state-of-the-art for continental-scale modelling, it is rather coarse for precise overlays with road segments. To mutually compare countries, we uniformly applied the 1:100 year flood maps without flood protection in the random sampling, thereby implicitly assuming that dikes will fail during the 1:100 year river flood. This is a reasonable average for Europe (Scussolini et al., 2016), but countries like Germany and The Netherlands have higher protection standards, whereas others like Albania and Bulgaria have lower standards. Moreover, inundation of a road segment does not necessarily mean that the road is completely destroyed, or even that it is completely inaccessible for a substantial time (Pregnolato et al., 2017, Loreti et al., 2022), cf. S4.7. Another complicating factor is that the weakest spots in the network might have already been floodproofed, without being noticed in our approach (cf. van Ginkel et al., 2021b). From a manual inspection of outlier events in Austria, we learned that roughly half of the outliers are actual points of concern, whereas the other half are probably model artefacts (Scoccimarro et al., 2020). In summary, we expect to have overestimated the susceptibility of the network in the random sampling, and to a lesser degree also in the guided sampling. Because of our worst-case assumptions, we have confidence in our conclusion that tipping points in the sense of 'percolation thresholds' are extremely to happen on the national scale as a result of river floods.

There is abundant room for further refinement of the methodological approach. On the hazard side, it would be valuable to reproduce the study with higher-resolution and fully event-based, multi-hazard flood data (cf. Loreti et al., 2022), because our elementary explorations for guided sampling in Germany already result in different results. There also is abundant room for further research on the impacts of compound hazards; during the July 2021 Western European floods we observed that pluvial floods, fluvial floods, and landslides combined, may locally have detrimental impact on the road network (Koks et al., 2021, under review). Concerning trip generation, an additional complexity could be to add weighing factors on origin–destination pairs, for example with a gravity model that puts additional weight on short-distance trips between regions with large economic activity (de Dios Ortúzar and Willumsen, 2009). Another refinement would be to add a metric that reflects the network capacity reduction when some but not all

routes between two regions are disrupted, this could serve as a simple proxy for the resulting traffic congestion (see Dong et al., 2022). Further work can extend the scope to multimodal networks. Our open-access model framework (see data and code availability) can be relatively easily transferred to the open rail network data in OpenStreetMap. More demanding, but highly relevant, would be an analysis of entire multi-modal trade corridors (such as the European TEN-T, Goldmann and Wessel, 2020), including the rail, road, and waterways network infrastructure. A promising advancement would be to explicitly include the (flood-prone) inland freight terminals and ports, as critical bottlenecks with possibly large non-linear impacts on transport flows.

6. Conclusion

This study identified many likely, unfavourable combinations of flood events that may qualify as socio-economic tipping points for some actors at specific spatial scales. In small mountainous countries like Slovenia, Macedonia and Albania, the 5% least favourable small-scale 1:100 year floods may disrupt 32 to 41% of the preferred routes between major economic regions, probably causing severe traffic disruptions beyond societal and legal acceptability thresholds, requiring a transformative response from national road operators. Other relatively vulnerable countries are Greece, Norway, Croatia, Serbia, Latvia and Austria. Explanatory variables that contribute to smaller robustness are large flood exposure, an unequal ratio between country length and width, mountains, and main corridors being located in the floodplains of rivers. Larger countries like Germany, Spain and France tend to have a more robust national network but suffer from the bias that local weaknesses are disguised in nationwide metrics.

At the same time, this study showed that in European countries, river floods are unlikely to cause tipping points in the sense of nationwide fragmentation of the network in isolated clusters (percolation points).

Despite its exploratory nature, this study offers policy-relevant insight. International decision makers such as investment banks and the European Commission can use the characterisation of network robustness to inform climate adaptation policies. The study sheds light on the system-of-system relations between physical infrastructure failure and national tipping-point like socio-economic impacts. As such, it is a relatively easy way explore the benefits of 'interoperable' adaption options, from asset to national scale (Vercruysse et al., 2019). Compared to traffic and macro-economic models, our model is relatively simple which could be useful for large-scale integral flood risk studies, which can use it to inventorize the impact of road and other network disruptions. National road operators can benefit from the inventory of disruptive outlier events, which can be traced back to the level of individual road segments. Further investigation of these points may result in quick wins for enhancing network robustness.

When accounting for the spatial correlation between concurrent river floods, the nationwide impacts in Germany strongly decreased. Therefore, more research with high resolution and event-based hazard data is needed to investigate if the risk of these socio-economic tipping points indeed is substantial. Our results do show that many countries have some regions that could become poorly accessible during river floods, which arguably is a tipping point at the regional scale. This finding contributes to our understanding of the potential of river floods to cause socio-economic tipping points; apparently, these are more likely to happen on smaller spatial scales.

The methodological merits of percolation analysis for supporting climate adaptation policy lie in its ability to quickly identify hotspots and provide insight into large-scale network robustness, for a large number of scenarios. Upon careful interpretation of the results, percolation analysis can be considered a useful tool for exploring many disruption scenarios, in some of which the network robustness may be severely challenged.

7. Data and code availability

The model code and data can be retrieved from https://doi.org/10.5281/zenodo.6587266.

Author contributions

KCHvG, EEK, and FdG conceptualised the study, developed the code, and visualised and interpreted the results. VDN and LA prepared the guided percolation flood hazard data. KCHvG and EEK wrote the initial manuscript. All authors reviewed, edited, and approved the manuscript.

Funding

This paper has received funding from the European Union's Horizon 2020 research and innovation programme under grant agreement No 776479 for the project CO-designing the Assessment of Climate CHange costs. https://www.coacch.eu/ EEK received funding from the EU Horizon-2020 project RECEIPT, grant No 820712; and the Dutch Research Council (NWO), grant No VI. Veni.194.033.

Declaration of Competing Interest

The authors declare that they have no known competing financial interests or personal relationships that could have appeared to influence the work reported in this paper.

Acknowledgements

We thank Ana Laura Costa, Ad Jeuken and Amine Aboufirass for their role in the conceptualization and coding of an early version of the analysis.

Appendix A. Supplementary material

Supplementary data to this article can be found online at https://doi.org/10.1016/j.trd.2022.103332.

References

Abdulla, B., Mostafavi, A., Birgisson, B., 2019. Characterization of the Vulnerability of Road Networks to Fluvial Flooding Using Network Percolation Approach. In: Computing in Civil Engineering 2019. American Society of Civil Engineers, Reston, VA, pp. 428–435. https://doi.org/10.1061/9780784482445.055.

Alfieri, L., Feyen, L., Dottori, F., Bianchi, A., 2015. Ensemble flood risk assessment in Europe under high end climate scenarios. Glob. Environ. Chang. 35, 199–212. https://doi.org/10.1016/j.gloenvcha.2015.09.004.

Arcaute, E., Molinero, C., Hatna, E., Murcio, R., Vargas-Ruiz, C., Masucci, A.P., Batty, M., 2016. Cities and regions in Britain through hierarchical percolation. R. Soc. Open Sci. 3 (4), 150691. https://doi.org/10.1098/rsos.150691.

Bles, T.; van Muiswinkel, K. Stress testing the Dutch national highway network. Proceedings of the 2nd International Conference on Resilience to Natural Hazards and Extreme Weather Events - Transportation Resilience 2019, Washington, DC, USA, November 13-15 2019.

Csardi, G., Nepusz, T., 2006. The igraph software package for complex network research. InterJournal, complex systems 1695 (5), 1–9.

de Dios Ortúzar, J., Willumsen, L.G., 2009. Modelling transport, third ed. John Wiley & Sons.

Dong, S., Mostafizi, A., Wang, H., Gao, J., Li, X., 2020a. Measuring the Topological Robustness of Transportation Networks to Disaster-Induced Failures: A Percolation Approach. J. Infrastruct. Syst. 26 (2), 04020009. https://doi.org/10.1061/(ASCE)IS.1943-555X.0000533.

Dong, S., Wang, H., Mostafizi, A., Song, X., 2020b. A network-of-networks percolation analysis of cascading failures in spatially co-located road-sewer infrastructure networks. Phys. A Stat. Mech. its Appl. 538, 122971. https://doi.org/10.1016/j.physa:2019.122971.

Dong, S., Gao, X., Mostafavi, A., Gao, J., 2022. Modest flooding can trigger catastrophic road network collapse due to compound failure. Commun. Earth Environ. 3, 38. https://doi.org/10.1038/s43247-022-00366-0.

Dottori, F., Mentaschi, L., Bianchi A., Alfieri, L., Feyen, L., 2021, under review. Adaptation is cost-effective to offset rising river flood risk in Europe. https://doi.org/10.21203/rs.3.rs-519118/v1.

Eurostat, 2016. The NUTS Nomenclature of territorial units for statistics. Available from http://ec.europa.eu/eurostat.

Filatova, T., Polhill, J.G., van Ewijk, S., 2016. Regime shifts in coupled socio-environmental systems: Review of modelling challenges and approaches. Environ. Model. Softw. 75, 333–347. https://doi.org/10.1016/j.envsoft.2015.04.003.

Fournier Gabela, J.G., Sarmiento, L., 2020. The effects of the 2013 floods on Germany's freight traffic. Transp. Res. Part D Transp. Environ. 82, 102274. https://doi.org/10.1016/j.trd.2020.102274.

Gavrilović, L., Milanović Pešić, A., Urošev, M., 2012. A hydrological analysis of the greatest floods in serbia in the 1960–2010 period. Carpathian J. Earth Environ. Sci. 7, 107–116.

GEER Geotechnical Extreme Events Reconnaissance, 2021 (in preparation), 2021 West European Floods, doi: https://doi.org/10.18118/G6XXXX.

van Ginkel, K.C.H., Haasnoot, M., Botzen, W.J.W., 2021a, preprint. A framework for identifying climate change induced socio-economic tipping points. https://doi.org/10.2139/ssrn.3935775.

van Ginkel, K.C.H., Botzen, W.J.W., Haasnoot, M., Bachner, G., Steininger, K.W., Hinkel, J., Watkiss, P., Boere, E., Jeuken, A.d., de Murieta, E.S., Bosello, F., 2020. Climate change induced socio-economic tipping points: review and stakeholder consultation for policy relevant research. Environ. Res. Lett. 15 (2), 023001. https://doi.org/10.1088/1748-9326/ab6395.

van Ginkel, K.C.H., Dottori, F., Alfieri, L., Feyen, L., Koks, E.E., 2021b. Flood risk assessment of the European road network. Nat. Hazards Earth Syst. Sci. 21 (3), 1011–1027. https://doi.org/10.5194/nhess-21-1011-202110.5194/nhess-21-1011-2021-supplement.

Goldmann, K., Wessel, J., 2020. TEN-T corridors – Stairway to heaven or highway to hell? Transp. Res. Part A Policy Pract. 137, 240–258. https://doi.org/10.1016/j.tra.2020.04.010.

de Grave, P., Slager, K., Wagenaar, D., van Marle, M., van Ginkel, K., 2020. Impact regionale overstromingen op hoofdwegennet (in Dutch). Deltares report, 11205243–006-BGS-0001.

Global Runoff Data Centre. River Discharge Data, 2020. https://www.bafg.de/GRDC/EN/Home/homep age_node.html, accessed 4 August 2020.

Hallegatte, S., Rentschler, J., Rozenberg, J., 2019. Lifelines: The Resilient Infrastructure Opportunity. World Bank, Washington DC. https://doi.org/10.1596/978-1-4648-1430-3.

IPCC, 2014. Climate Change 2014: Impacts, Adaptation, and Vulnerability. Part B: Regional Aspects. Cambridge University Press, Cambridge, United Kingdom and New York, USA.

Jain, V., Sharma, A., Subramanian, L., 2012. Road traffic congestion in the developing world. Proc. 2nd ACM Symp. Comput. Dev. DEV 2012. https://doi.org/10.1145/2160601.2160616.

Johnston, I., Murphy, W., Holden, J., 2021. A review of floodwater impacts on the stability of transportation embankments. Earth-Science Rev. 215, 103553. https://doi.org/10.1016/j.earscirev.2021.103553.

Koks, E.E., Rozenberg, J., Zorn, C., Tariverdi, M., Vousdoukas, M., Fraser, S.A., Hall, J.W., Hallegatte, S., 2019. A global multi-hazard risk analysis of road and railway infrastructure assets. Nat. Commun. 10, 1–11. https://doi.org/10.1038/s41467-019-10442-3.

Koks, E., Van Ginkel, K., Van Marle, M., Lemnitzer, A., 2021. Brief Communication: Critical Infrastructure impacts of the 2021 mid-July western European flood event. Nat. Hazards Earth Syst. Sci. Discuss. https://doi.org/10.5194/nhess-2021-394 in review [preprint].

Kopp, R.E., Shwom, R.L., Wagner, G., Yuan, J., 2016. Tipping elements and climate-economic shocks: Pathways toward integrated assessment. Earth's Futur. 4 (8), 346–372. https://doi.org/10.1002/2016EF000362.

Kreienkamp, F., Philip, S.Y., Tradowsky, J.S., Kew, S.F., Lorenz, P., Arrighi, J., Belleflamme, A., Bettmann, T., Caluwaerts, S., Chan, S.C., Ciavarella, A., De Cruz, L., de Vries, H., Demuth, N., Ferrone, A., Fischer, E.M., Fowler, H.J., Goergen, K., Heinrich, D., Henrichs, Y., Lenderink, G., Kaspar, F., Nilson, E., Otto, F.E., 2021. Rapid Attribution of Heavy Rainfall Events Leading to the Severe Flooding in Western Europe During July 2021. World Weather Attribution.

Loreti, S., Ser-Giacomi, E., Zischg, A., Keiler, M., Barthelemy, M., 2022. Local impacts on road networks and access to critical locations during extreme floods. Sci. Rep. 12, 1552. https://doi.org/10.1038/s41598-022-04927-3.

Milkoreit, M., Hodbod, J., Baggio, J., Benessaiah, K., Calderón-Contreras, R., Donges, J.F., Mathias, J.-D., Rocha, J.C., Schoon, M., Werners, S.E., 2018. Defining tipping points for social-ecological systems scholarship—an interdisciplinary literature review. Environ. Res. Lett. 13 (3), 033005. https://doi.org/10.1088/1748-9326/aaaa75.

Mulholland, E., Alfieri, L., Dottori, F., Mentaschi, L., Ciscar, J. C. and Feyen, L. 2021, "Increased river flood risk to European transport infrastructures with global warming", Environmental Research Letters, under review.

van Nes, E.H., Arani, B.M.S., Staal, A., van der Bolt, B., Flores, B.M., Bathiany, S., Scheffer, M., 2016. What Do You Mean, 'Tipping Point'? Trends Ecol. Evol. 31 (12), 902–904. https://doi.org/10.1016/j.tree.2016.09.011.

Nguyen, V.D., Metin, A.D., Alfieri, L., et al., 2020. Biases in national and continental flood risk assessments by ignoring spatial dependence. Sci. Rep. 10, 19387. https://doi.org/10.1038/s41598-020-76523-2.

Nicklin, L., Dieperink, L., 2019. Understanding the Costs of Inaction–An Assessment of Pluvial Flood Damages in Two European Cities. Water 11 (4), 801. https://doi.org/10.3390/w11040801.

OpenStreetMap contributors (2020). Available at: http://openstreetmap.org, last accessed 1 December 2020.

Palko, K., Lemmen, D.S. (Eds.), 2017. Climate risks and adaptation practices for the Canadian transportation sector 2016. Government of Canada, Ottawa, ON.

Pedrozo-Acuña, A., Moreno, G., Mejía-Estrada, P., Paredes-Victoria, P., Breña-Naranjo, J.A., Meza, C., 2017. Integrated approach to determine highway flooding and critical points of drainage. Transp. Res. Part D Transp. Environ. 50, 182–191. https://doi.org/10.1016/j.trd.2016.11.004.

Pregnolato, M., Ford, A., Wilkinson, S.M., Dawson, R.J., 2017. The impact of flooding on road transport: A depth-disruption function. Transp. Res. Part D Transp. Environ. 55, 67–81. https://doi.org/10.1016/j.trd.2017.06.020.

Radicchi, F., 2015. Predicting percolation thresholds in networks. Phys. Rev. E - Stat. Nonlinear, Soft Matter Phys. 91, 1–5. https://doi.org/10.1103/PhysRevE.91.010801.

Russill, C., Lavin, C., 2012. Tipping point discourse in dangerous times. Can. Rev. Am. Stud. 42 (2), 142–163. https://doi.org/10.3138/cras.42.2.142.

Scussolini, P., Aerts, J.C.J.H., Jongman, B., Bouwer, L.M., Winsemius, H.C., De Moel, H., Ward, P.J., 2016. FLOPROS: an evolving global database of flood protection standards. Nat. Hazards Earth Syst. Sci. 16, 1049–1061. https://doi.org/10.5194/nhess-16-1049-2016.

Scoccimarro, E., Steininger, K.W., Watkiss, P.. Boere, E., Hunt, A., Linke, D., Grossmann, W., Tesselaar, M., Williges, K., Ignjacevic, P., Jeuken, A., van Ginkel, K., Costa, A.L., Groen, F., Peano, P., Fogli, G., Ruggieri, P., Chaves Montero, MdM., 2020. D3.2. Tipping point likelihood in the SSP/RCP space. Deliverable of the H2020 COACCH project. Availabe from www.coacch.eu.

Vercruysse, K., Dawson, D.A., Wright, N., 2019. Interoperability: A conceptual framework to bridge the gap between multifunctional and multisystem urban flood management. J. Flood Risk Manag. 12 (S2) https://doi.org/10.1111/jfr3.v12.S210.1111/jfr3.12535.

Wang, C., Yu, X., Liang, F., 2017. A review of bridge scour: mechanism, estimation, monitoring and countermeasures. Nat. Hazards 87 (3), 1881–1906. https://doi.org/10.1007/s11069-017-2842-2.

Wang, T., Qu, Z., Yang, Z., Nichol, T., Clarke, G., Ge, Y.-E., 2020. Climate change research on transportation systems: Climate risks, adaptation and planning. Transp. Res. Part D Transp. Environ. 88, 102553. https://doi.org/10.1016/j.trd.2020.102553.

Wang, W., Yang, S., Stanley, H.E., Gao, J., 2019. Local floods induce large-scale abrupt failures of road networks. Nat. Commun. 10, 2114. https://doi.org/10.1038/s41467-019-10063-w.

Zhang, N., Alipour, A., 2020. Multi-scale robustness model for highway networks under flood events. Transp. Res. Part D Transp. Environ. 83, 102281 https://doi.org/10.1016/j.trd.2020.1.

Further reading

Schneider, C.M., Moreira, A.A., Andrade, J.S., Havlin, S., Herrmann, H.J., 2011. Mitigation of malicious attacks on networks. Proc. Natl. Acad. Sci. U. S. A. 108 (10), 3838–3841. https://doi.org/10.1073/pnas.1009440108.